Evidence That Isoprene Emission Is Not Limited by Cytosolic Metabolites. Exogenous Malate Does Not Invert the Reverse Sensitivity of Isoprene Emission to High [CO_2][1]

Bahtijor Rasulov,[a,b] Eero Talts,[a] Irina Bichele,[c] and Ülo Niinemets[a,d,2]

[a]Institute of Agricultural and Environmental Sciences, Estonian University of Life Sciences, 51014 Tartu, Estonia
[b]Institute of Technology, University of Tartu, Tartu 50411, Estonia
[c]Institute of Physics, University of Tartu, 50411 Tartu, Estonia
[d]Estonian Academy of Sciences, 10130 Tallinn, Estonia

ORCID IDs: 0000-0001-5178-8617 (B.R.); 0000-0002-8093-6444 (E.T.); 0000-0002-9493-0094 (I.B.); 0000-0002-3078-2192 (Ü.N.).

Isoprene is synthesized via the chloroplastic 2-*C*-methyl-D-erythritol 4-phosphate/1-deoxy-D-xylulose 5-phosphate pathway (MEP/DOXP), and its synthesis is directly related to photosynthesis, except under high CO_2 concentration, when the rate of photosynthesis increases but isoprene emission decreases. Suppression of MEP/DOXP pathway activity by high CO_2 has been explained either by limited supply of the cytosolic substrate precursor, phospho*enol*pyruvate (PEP), into chloroplast as the result of enhanced activity of cytosolic PEP carboxylase or by limited supply of energetic and reductive equivalents. We tested the PEP-limitation hypotheses by feeding leaves with the PEP carboxylase competitive inhibitors malate and diethyl oxalacetate (DOA) in the strong isoprene emitter hybrid aspen (*Populus tremula* × *Populus tremuloides*). Malate feeding resulted in the inhibition of net assimilation, photosynthetic electron transport, and isoprene emission rates, but DOA feeding did not affect any of these processes except at very high application concentrations. Both malate and DOA did not alter the sensitivity of isoprene emission to high CO_2 concentration. Malate inhibition of isoprene emission was associated with enhanced chloroplastic reductive status that suppressed light reactions of photosynthesis, ultimately leading to reduced isoprene substrate dimethylallyl diphosphate pool size. Additional experiments with altered oxygen concentrations in conditions of feedback-limited and non-feedback-limited photosynthesis further indicated that changes in isoprene emission rate in control and malate-inhibited leaves were associated with changes in the share of ATP and reductive equivalent supply for isoprene synthesis. The results of this study collectively indicate that malate importantly controls the chloroplast reductive status and, thereby, affects isoprene emission, but they do not support the hypothesis that cytosolic metabolite availability alters the response of isoprene emission to changes in atmospheric composition.

Isoprene is one of the main reactive volatiles released by plants that dominates atmospheric oxidative processes over a large part of the globe (Guenther et al., 2012; Guenther, 2013). Thus, understanding the controls of isoprene emission is the key for constructing predictive models capable of reliable estimation of isoprene source strength in current and future climates (Monson et al., 2012; Grote et al., 2013). Furthermore, monitoring isoprene emissions can serve as a simple noninvasive means to gain insight into the relationships between photosynthetic processes and plant isoprenoid synthesis, especially into regulation of the chloroplastic 2-*C*-methyl-D-erythritol 4-phosphate/1-deoxy-D-xylulose 5-phosphate (MEP/DOXP) pathway that is responsible for the synthesis of isoprene, monoterpenes, diterpenes such as gibberllic acids and phytol residue in chlorophylls, and tetraterpenes such as carotenoids (Trowbridge et al., 2012; Ghirardo et al., 2014).

Plant isoprene emission is strongly correlated with foliage net assimilation rate through different light levels, but the responses of isoprene emission and net assimilation to changes in ambient CO_2 concentration differ, with net assimilation increasing hyperbolically and isoprene emission decreasing with rising CO_2 concentration (Loreto and Sharkey, 1990; Wilkinson et al., 2009; Monson et al., 2012; Li and Sharkey, 2013b). There is still no consensus regarding the mechanisms leading to the contrasting responses of photosynthesis and isoprene emission to CO_2. The first reaction in the MEP/DOXP pathway is the condensation of glyceraldehyde-3-phosphate (GAP) and

[1] The group's research on factors controlling plant volatile release is financially supported by the Estonian Ministry of Science and Education (institutional grant IUT-8-3), the European Research Council (advanced grant 322603, SIP-VOL+), and the European Commission through the European Regional Development Fund (Center of Excellence EcolChange).

[2] Address correspondence to ylo.niinemets@emu.ee.

The author responsible for distribution of materials integral to the findings presented in this article in accordance with the policy described in the Instructions for Authors (www.plantphysiol.org) is: Ülo Niinemets (ylo.niinemets@emu.ee).

B.R. and Ü.N. posed the hypothesis and planned the study; B.R., E.T., and I.B. carried out the experiments; B.R. and E.T. analyzed the data; B.R. and Ü.N. drafted the first version of the article, and all authors contributed to and approved the final version of the article.

www.plantphysiol.org/cgi/doi/10.1104/pp.17.01463

pyruvate, leading to the formation of 1-deoxy-D-xylulose 5-phosphate. GAP comes directly from the Calvin cycle, but the origin of chloroplastic pyruvate has remained enigmatic. In particular, $^{13}CO_2$-labeling studies indicate that isoprene is not fully labeled even after prolonged labeling (up to approximately 90%; Delwiche and Sharkey, 1993) and that that the carbon fragments coming from pyruvate show slower labeling (Trowbridge et al., 2012). This evidence has been interpreted as indicative of a cytosolic source for pyruvate (Rosenstiel et al., 2003; Trowbridge et al., 2012). In particular, it has been suggested that the main source of chloroplastic pyruvate is the cytosolic phospho*enol*pyruvate (PEP) that is transported through a specific carrier to chloroplasts and converted to pyruvate there (Rosenstiel et al., 2003; Wiberley et al., 2005; Banerjee and Sharkey, 2014; Potosnak, 2014). As GAP is readily available at high CO_2 concentration, the PEP-limitation hypothesis of isoprene emission suggests that it is the transport of PEP into chloroplasts that constrains isoprene emission at high CO_2 concentration (Fig. 1; Rosenstiel et al., 2003; Potosnak, 2014). Specifically, it has been suggested that, under high CO_2 concentration, PEP carboxylase (PEPC) activity increases due to increases in cytosolic bicarbonate concentration and that this draws down the cytosolic PEP level and reduces its import into chloroplast (Fig. 1; Rosenstiel et al., 2003). Because PEP is transported into the chloroplast by an anion transporter in exchange for inorganic phosphate (Flügge et al., 2011), PEP limitation of isoprene emission has also been associated with conditions of feedback-limited photosynthesis when low chloroplastic phosphate levels curb the rate of photosynthesis, typically under high CO_2 and low oxygen concentrations (Li and Sharkey, 2013b; Banerjee and Sharkey, 2014).

The synthesis of isoprene as a highly reduced molecule requires more ATP and reductive equivalents than the synthesis of the first products of photosynthesis; thus, it has been suggested that isoprene emission is limited by the rate of photosynthetic electron transport (Niinemets et al., 1999b; Rasulov et al., 2009b). This suggestion has been supported by the evidence that short-term changes in isoprene emission were correlated with leaf ATP concentration (Loreto and Sharkey, 1993); by data showing strong covariation in primary isoprene substrate, DMADP, and photosynthetic electron transport rate through light and CO_2 and oxygen concentrations (Rasulov et al., 2009b); and by the demonstration of simultaneous oscillatory dynamics in isoprene emission, photosynthetic electron transport, and photosynthesis rate induced in conditions when photosynthesis is feedback limited (Rasulov et al., 2016). According to the mechanism of limitation of isoprene emission by the availability of energetic and/or reductive equivalents, the MEP/DOXP pathway has a high effective Michaelis-Menten constant for energetic and/or reductive cofactors, implying that the synthesis of DMADP is very sensitive to reductions in the pool sizes of ATP and/or NADPH. Under conditions of high CO_2, the rate of photosynthesis is increased, but its potential rate is curbed by limited regeneration of ribulose-1,5-bisphosphate (RuBP; Farquhar et al., 1980). Thus, under these conditions, ATP, NADPH, and RuBP pool sizes are reduced (although their turnover is high; Badger et al., 1984; Dietz et al., 1984; Heber et al., 1986; von Caemmerer, 2000), leading to a reduced rate of DMADP synthesis and reduced isoprene emission (Rasulov et al., 2009b, 2016).

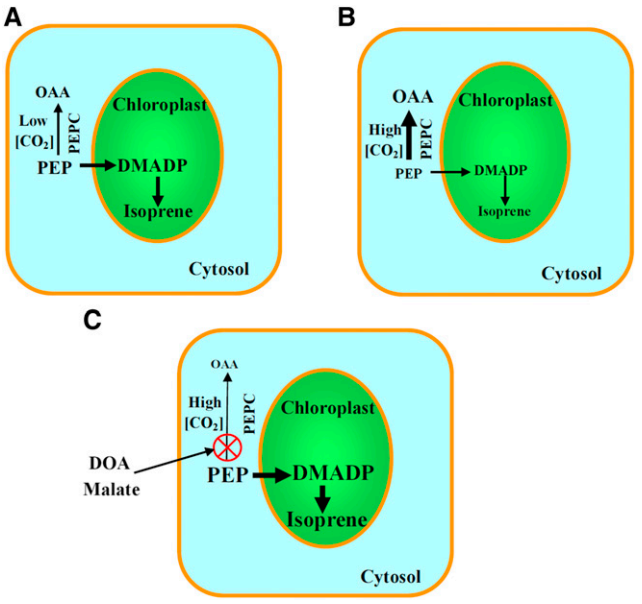

Figure 1. Isoprene emission rate decreases with increasing ambient CO_2 concentration (C_a), but photosynthesis increases with increasing C_a. Illustration of the hypothesis of how high ambient CO_2 might inhibit plant isoprene emission. The immediate isoprene precursor dimethylallyl diphosphate (DMADP) is synthesized in chloroplasts via the MEP/DOXP pathway that starts with the condensation of pyruvate and GAP. GAP for DMADP synthesis comes directly from photosynthesis, but it is currently still unclear what is the chloroplastic source of pyruvate. It has been suggested that pyruvate can be synthesized directly in chloroplasts (Sharkey et al., 2008; Rasulov et al., 2011), while others have postulated the necessary import of the pyruvate precursor PEP via a specific carrier into the chloroplasts (Rosenstiel et al., 2003; Wilkinson et al., 2009; Monson et al., 2012). It has further been suggested that the rate of PEP transport into chloroplasts is limited by cytosolic PEP concentration that is under the control of PEPC (Rosenstiel et al., 2003; Wilkinson et al., 2009; Monson et al., 2012). Under low C_a (A), a smaller fraction of cytosolic PEP is converted to oxalacetate (OAA), while the fraction increases under higher C_a (B), supposedly leading to a lower rate of PEP transport into the chloroplasts, curbing the rate of isoprene synthesis. If so, feeding the leaves with malate that is in equilibrium with OAA, but that also serves as an inhibitor of PEPC, or feeding with the specific PEPC inhibitor diethyl oxalacetate (DOA) should result in a greater PEP pool and, thus, abolish the effect of high CO_2 concentration on isoprene emission.

Although the PEP-limitation hypothesis is plausible, there is currently primarily indirect evidence for its support (Rosenstiel et al., 2003; Trowbridge et al., 2012; Potosnak, 2014). One key piece of evidence in support of the partial cytosolic origin of isoprene intermediates, incomplete ^{13}C labeling of isoprene in $^{13}CO_2$-labeling experiments, was recently suggested to be a general feature of Calvin cycle products due to an operative

Glc-6-P shunt around the Calvin cycle (Sharkey and Weise, 2016). Thus, the main direct support comes from PEPC inhibitor experiments where PEPC inhibition was associated with a certain increase in isoprene emission (Fig. 1; Rosenstiel et al., 2003). However, in these experiments, the rate of photosynthesis also decreased in PEPC-inhibited leaves (Rosenstiel et al., 2003), implying profound metabolic modifications, including modifications in leaf energetic status, but insufficient physiological information was obtained to link the changes in isoprene emission directly to improved substrate availability. To test the hypothesis of the regulatory role of PEPC, in this study, we used leaf feeding with malate, which is a competitive inhibitor of PEPC (Wedding and Black, 1986; Asai et al., 2000; Moraes and Plaxton, 2000; Chinthapalli et al., 2003). Furthermore, exogenous malate can also enter directly into metabolism via gluconeogenesis in the cytosol, enhancing metabolic pressure for the formation of PEP (malate < OAA < PEP), thereby contributing directly to the increase of cytosolic PEP concentration. Thus, we expected that, in conditions of high CO_2 concentration, the cytosolic PEP level would increase and that this would reverse the reduction in CO_2-dependent isoprene emission (Fig. 1). As a complementary test, the experiments were repeated with diethyl oxalacetate (DOA), another PEPC competitive inhibitor (Walker and Edwards, 1990). Apart from modifications in CO_2 concentration, the responses of photosynthesis and isoprene emission to alterations in ambient oxygen concentration were studied to test the possible effect of PEP availability under feedback-limited conditions. The results collectively suggest that cytosolic PEP availability is not responsible for the reduction in isoprene emission under high CO_2 concentration and in feedback-limited conditions. Rather, malate-feeding experiments supported the view that the CO_2 and oxygen dependencies of isoprene emission are driven by alterations in the share of reductive equivalents available for the MEP/DOXP pathway.

RESULTS

Effects of Malate Feeding on Foliage Photosynthetic Characteristics

The initial rapid response to malate feeding was a moderate increase of stomatal openness, for approximately 50 to 200 s after the start of malate feeding, followed by a continuous decline until stabilization at approximately 1,500 s after the start of feeding (Figs. 2 and 3; Table I). The quantum yield of PSII and net assimilation rate initially declined at a slow rate between approximately 150 and 300 s after the start of feeding, followed by a fast rate of reduction between approximately 300 and 400 s, succeeded again by a slower rate of decrease (Fig. 2). The PSII quantum yield stabilized at approximately 60% to 65%, and the net assimilation rate at approximately 40% to 50% of the corresponding initial values, by approximately 1,500 s after the start of feeding

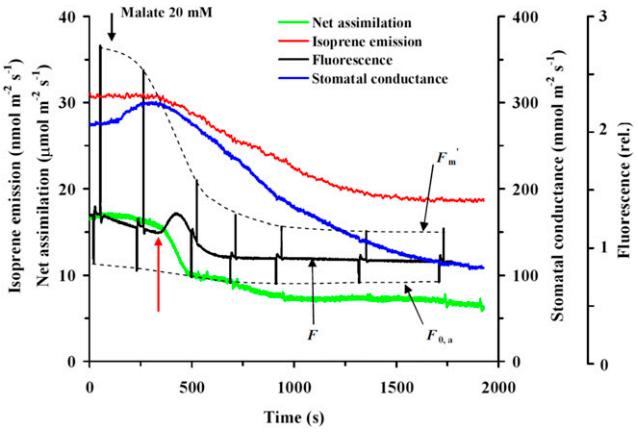

Figure 2. Characteristic modifications in leaf isoprene and net assimilation rates, stomatal conductance to water vapor, and chlorophyll fluorescence upon application of 20 mM malate solution in hybrid aspen (clone H200). The measurements were conducted at the standard conditions of leaf temperature of 30°C, light intensity of 700 μmol m^{-2} s^{-1}, and leaf chamber CO_2 concentration of 400 μmol mol^{-1}. The start of inhibitor application is shown by the black arrow. F_m' denotes the maximum chlorophyll fluorescence yield and $F_{0,a}$ the minimum fluorescence yield in a partly relaxed state achieved by illuminating the leaves with far-red light (150 μmol m^{-2} s^{-1}). The red arrow indicates the postulated transition to the reverse mode of the malate shuttle.

(Fig. 2; Table I). At this time, the intercellular CO_2 concentration (C_i) had only decreased by approximately 15% (Table I), indicating significant nonstomatal limitations of photosynthesis. In fact, the apparent maximum carboxylase activity of Rubisco (V_{cmax}) also declined by approximately 35% to 40%, similar to changes in the quantum yield of PSII (Table I). Different from all other photosynthetic characteristics, the dark respiration rate had increased by approximately 2-fold and the post-illumination CO_2 burst (an estimate of photorespiration rate) by 1.7-fold by the end of the treatment (Table I).

Changes in Leaf Isoprene Emission Characteristics in Malate-Inhibited Leaves

The isoprene emission rate started to decrease approximately 250 s after the start of malate feeding and decreased continuously to approximately 60% of the initial value by 1,500 s after the start of feeding (Fig. 2; Table II). The reduction in isoprene emission was paralleled by even stronger decreases in DMADP pool size, stabilizing at a level of 40% of the initial value (Table II). In contrast, the dark pool size (the pool of MEP/DOXP pathway intermediates prior to DMADP, consisting primarily of 2-C-methyl-D-erythritol 2,4-cyclodiphosphate [MEcDP]), the initial slope of the DMADP pool size and isoprene rate relationship (isoprene synthase rate constant), and the apparent maximum capacity of isoprene synthase were unaffected by malate feeding, but the apparent Michaelis-Menten constant was reduced somewhat in malate-fed leaves (Table II). Across control and malate-

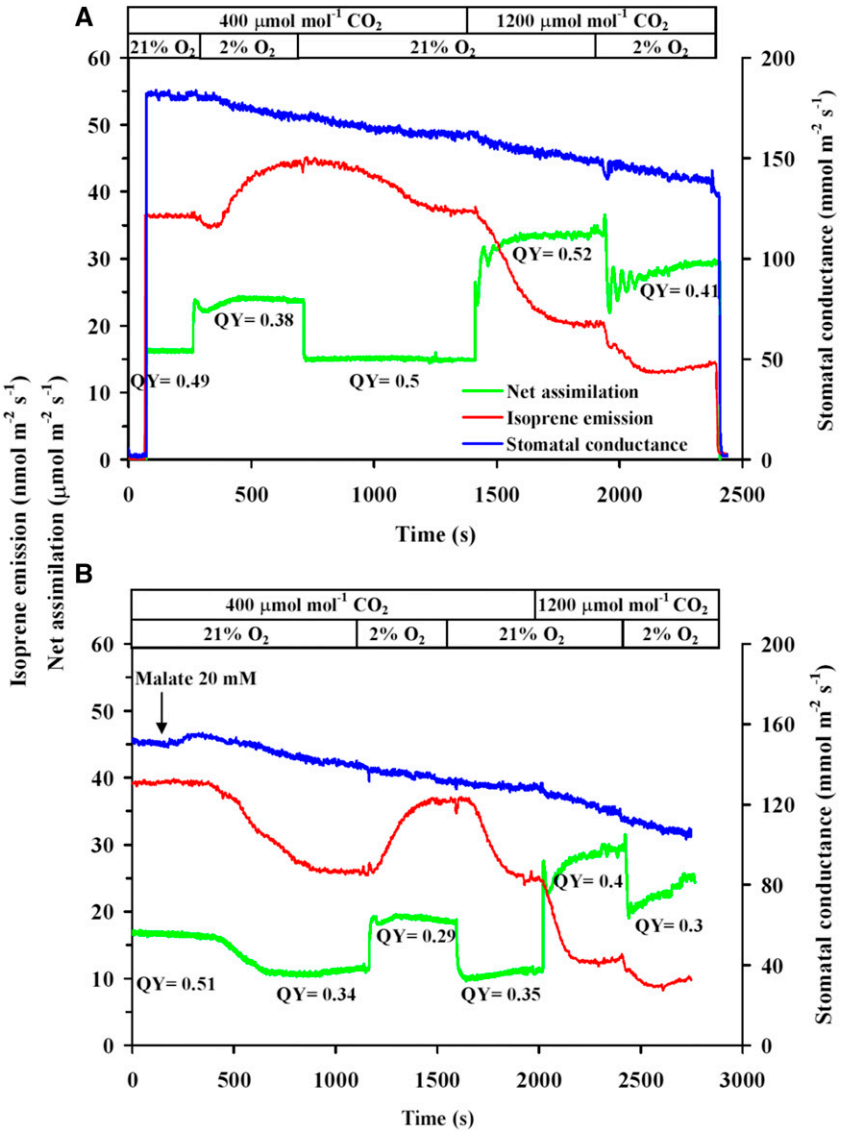

Figure 3. Kinetic modifications in isoprene emission and net assimilation rates and stomatal conductance upon modifications in atmospheric CO_2 and oxygen concentrations in control leaves (A) and in leaves during malate inhibition (B) in hybrid aspen. QY denotes the effective quantum yield of PSII for different steady states at different gas compositions. The first transition in gas composition in leaves fed with malate (B; reduction of oxygen concentration from 21% to 2% (v/v) under ambient CO_2 concentration of 400 μmol mol^{-1}) was carried out once almost full inhibition of malate was achieved (i.e. net assimilation and isoprene emissions had reached a new steady state).

inhibited leaves, the isoprene emission rate and DMADP pool size at the ambient CO_2 concentration of 400 μmol mol^{-1} were strongly correlated with the effective PSII quantum yield ($r^2 = 0.98$ for isoprene emission and $r^2 = 0.78$ for DMADP pool size; $P < 0.01$ for both).

Modification of Kinetic Responses of Net Assimilation Rate and Isoprene Emission to CO_2 and Oxygen Concentrations by Malate Inhibition

In control leaves at the ambient CO_2 concentration of 400 μmol mol^{-1}, the reduction of oxygen concentration from 21% to 2% (v/v) resulted in rapid increases in net assimilation rate followed by a transient minor (Fig. 3A) to relatively large (Supplemental Fig. S1A) reduction until reaching again the higher steady-state level (Fig. 3A; Table III; Supplemental Fig. S1A). Different from photosynthesis, the initial decline in isoprene emission upon the decrease of oxygen concentration was generally greater, approximately 10% to 35% in different experiments, but the emission rate recovered under low oxygen, and in the steady state exceeded the rate at 21% oxygen by approximately 20% (Figs. 3A and 4; Table III; Supplemental Fig. S1). In malate-inhibited leaves, the responses to low oxygen under ambient CO_2 were similar, except that the initial reduction in isoprene emission was absent (Fig. 3B; Table III). In addition, the relative enhancement of both net assimilation rate and isoprene emission by low oxygen was greater in malate-inhibited leaves (approximately 30%–35% for both rates; compare Figs. 3 and 4; Table III).

In control leaves, a rapid increase in CO_2 concentration from 400 to 1,200 μmol mol^{-1} under ambient oxygen of 21% enhanced net assimilation rate by 40% to 60% and reduced isoprene emission rate by 50% to 60% (Figs. 3 and 4; Table III; Supplemental Fig. S1). The responses were analogous in malate-inhibited leaves, whereas, for the net assimilation rate, relative changes were

Table I. *Effects of leaf feeding with malate on foliage photosynthetic characteristics in hybrid aspen (clone H200)*

Characteristic	Control	Malate Treated
A_n (μmol m^{-2} s^{-1})	16.30 ± 0.43 a	7.70 ± 0.44 b
V_{cmax} (μmol m^{-2} s^{-1})	68.0 ± 1.6 a	43.0 ± 2.8 b
g_s (mmol m^{-2} s^{-1})	280 ± 10 a	102 ± 7 b
C_i (μmol mol^{-1})	303.8 ± 3.0 a	266 ± 7 b
R_D (μmol m^{-2} s^{-1})	1.63 ± 0.07 c	3.43 ± 0.42 a
R_B (μmol m^{-2} s^{-1})	3.06 ± 0.12 b	4.93 ± 0.28 a
QY (mol mol^{-1})	0.641 ± 0.013 a	0.428 ± 0.014 b

The standard conditions during the measurements were as follows: leaf temperature of 30°C, light intensity of 700 μmol m^{-2} s^{-1}, and leaf chamber CO_2 concentration of 400 μmol mol^{-1}. After steady-state conditions were established under these conditions, foliage photosynthetic characteristics were measured (control), the leaves were further fed for 40 min with malate solution (20 mM), and foliage photosynthetic characteristics were measured again (for kinetic changes in leaf photosynthetic characteristics during inhibitor application, see Fig. 2). R_B was measured immediately after leaf darkening and R_D when the gas-exchange rate in the dark had reached a steady state. The data are means ± SE of four to five replicate experiments with different leaves. SE was calculated as the sample SD divided by the square root of n, where n is the number of replicate experiments. Values followed by the same letter are not significantly different ($P > 0.05$) according to paired-samples Student's t test. A_n, Net CO_2 assimilation rate; V_{cmax}, apparent (C_i-based) maximum carboxylase activity of Rubisco; g_s, stomatal conductance for water vapor; C_i, intercellular CO_2 concentration; R_D, dark respiration rate; R_B, rate of CO_2 release at postillumination CO_2 burst (an estimate of the rate of photorespiration with a residual component of dark respiration remaining in light and a certain consumption of CO_2 due to the existing RuBP pool); QY, light-adapted (effective) quantum yield of PSII.

greater in malate-inhibited leaves, but for the isoprene emission rate, relative changes did not differ significantly among control and malate-inhibited leaves (Figs. 3B and 4; Table III).

In control leaves, a rapid reduction of oxygen concentration from 21% to 2% under high CO_2 concentration of 1,200 μmol mol^{-1} reduced both net assimilation and isoprene emission rates, whereas the transition from one steady-state level to the other proceeded through oscillatory dynamics for both net assimilation and isoprene emission rates (Fig. 3A; Supplemental Fig. S1). In malate-inhibited leaves, the responses were again qualitatively similar, except that the oscillations were absent (Fig. 3B). The relative reduction in net assimilation rate was greater for malate-inhibited leaves, but the relative reduction in isoprene emission was greater for control leaves (Table III).

Across all data, the relative change in net assimilation rate ($R_{c,A}$) and the relative change in isoprene emission rate ($R_{c,I}$) were correlated, whereas the change in $R_{c,I}$ at the given change in $R_{c,A}$ was less for oxygen concentration transitions (from 21% to 2%) than for CO_2 transitions (from 400 to 1,200 μmol mol^{-1} CO_2; Fig. 4). For both transitions, both $R_{c,A}$ and $R_{c,I}$ were greater for malate-inhibited leaves (Fig. 4).

Effects of the PEPC Inhibitor DOA on Foliage Photosynthesis and Isoprene and Acetaldehyde Emissions

Application of the PEPC inhibitor diethyl oxalacetate (DOA) at a concentration of 150 μM typically used in plant experiments (Magnin et al., 1997; Rosenstiel et al., 2003) and application of even a higher concentration of 500 μM did not influence net assimilation and isoprene emission rates, stomatal conductance, and effective quantum yield of PSII of hybrid aspen (*Populus tremula* × *Populus tremuloides*) leaves (Fig. 5, A and C). Furthermore, 150 and 500 μM DOA did not affect the inhibition of isoprene emission by high CO_2 concentration (Fig. 5A). However, both these concentrations resulted in enhanced emissions of acetaldehyde (Fig. 5B, for a sample kinetics of 150 μM DOA). Some inhibition of photosynthetic characteristics and isoprene emission was observed only at 20 mM DOA (i.e. at a concentration 100–200 times greater than shown previously to be effective in plants). The effect of these high DOA concentrations likely was nonspecific, as, surprisingly, DOA also resulted in enhanced stomatal conductance (Fig. 5).

Table II. *Modification of isoprene emission characteristics upon leaf feeding with malate in hybrid aspen (clone H200)*

Characteristic	Control	Malate Treated
I (nmol m^{-2} s^{-1})	30.4 ± 1.6 a	18.5 ± 0.7 b
DMADP pool (nmol m^{-2})	1,180 ± 60 a	470 ± 36 b
Dark pool (nmol m^{-2})	2,170 ± 190 a	2,700 ± 190 a
Rate constant (s^{-1})	0.0372 ± 0.0010 a	0.0358 ± 0.0016 a
V_{max} (nmol m^{-2} s^{-1})	69.5 ± 1.1 a	73 ± 6 a
K_m (nmol m^{-2})	2,038 ± 47 a	1,600 ± 90 b

Experimental treatments, measurement conditions, number of replicates, and statistical analyses were as in Table I. I, Isoprene emission rate; V_{max}, apparent capacity for isoprene synthase reaction in vivo; K_m, apparent Michaelis-Menten constant for isoprene synthase in vivo. The pool size of DMADP and the dark pool size (the pool of MEP/DOXP pathway intermediates prior to the 4-hydroxy-3-methylbut-2-enyl diphosphate synthase [HDS] and 4-hydroxy-3-methylbut-2-enyl diphosphate reductase [HDR] reactions) were estimated from the dark decay kinetics of isoprene emission (Rasulov et al., 2009a, 2011; Li et al., 2011). After switching off the light, integration of the rapid decay of isoprene emission, up to approximately 200 to 250 s after the darkening, corresponds to the DMADP pool size responsible for isoprene emission in the light. A second, dark-activated burst of isoprene emission occurs between approximately 250 and 600 s, and the integral of the second emission peak provides the size of the dark pool. Pairwise values of the DMADP pool size and the corresponding isoprene emission rates through the dark decay kinetics were used to determine the isoprene synthase rate constant (the initial slope of isoprene emission rate versus DMADP pool size) and apparent K_m and V_{cmax} values (Rasulov et al., 2014, 2015a).

Table III. *Relative changes (average ± SE) in net assimilation rate ($R_{c,A}$) and isoprene emission rate ($R_{c,I}$) in control and malate-inhibited hybrid aspen (clone H200) leaves upon transition from CO_2 concentrations of 400 to 1,200 μmol mol^{-1} and from oxygen concentrations of 21% to 2% at CO_2 concentrations of 400 and 1,200 μmol mol^{-1}*

Transition	$R_{c,A}$		$R_{c,I}$	
	Control	Malate Treated	Control	Malate Treated
400→1,200 μmol mol^{-1} CO_2, 21% oxygen	0.638 ± 0.006 a	0.737 ± 0.017 b	−0.574 ± 0.034 a	−0.614 ± 0.017 a
21%→2% oxygen, 400 μmol mol^{-1} CO_2	0.406 ± 0.015 a	0.555 ± 0.019 b	0.160 ± 0.008 a	0.257 ± 0.021 b
21%→2% oxygen, 1,200 μmol mol^{-1} CO_2	−0.146 ± 0.017 a	−0.200 ± 0.010 b	−0.376 ± 0.015 a	−0.242 ± 0.021 b

Experimental treatments, measurement conditions, number of replicates, and statistical analyses were as in Table I. $R_{c,A} = \Delta A/\bar{A}$ and $R_{c,I} = \Delta I/\bar{I}$, where ΔA and ΔI are differences between steady-state net assimilation and isoprene emission rates estimated before and after the change in leaf chamber gas composition, and $\bar{A}$ and $\bar{I}$ are averages for the two steady states (Rasulov et al., 2016).

DISCUSSION

Influence of Malate on Foliage Photosynthetic Activity

Malate feeding of hybrid aspen leaves resulted in reduced net assimilation rate and reduced stomatal conductance (Figs. 2 and 3; Table I; Supplemental Fig. S1). As the C_i was also reduced (Table I), the reduction in net assimilation rate was due to both stomatal and nonstomatal processes, as confirmed by simultaneous reductions in the apparent V_{cmax} and in the effective quantum yield of PSII (Figs. 2 and 3; Table I; Supplemental Fig. S1). A similar reduction of PSII activity and photosynthesis rate upon malate feeding has been observed in malate-fed rice (*Oryza sativa*) leaves, and this was associated with a reduction in the number of open PSII reaction centers (Cui et al., 2015).

In photosynthesizing leaves, malate participates in shuttling reductive equivalents from chloroplasts to cytosol via a malate/OAA shuttle, maintaining the necessary balance between chloroplastic NADPH and ATP levels (Scheibe et al., 1986; Scheibe, 1987; Fig. 6). Chloroplastic malate accumulation is expected to result in an enhanced chloroplastic NADPH/NADP$^+$ ratio as the result of reversal of the malate dehydrogenase reaction toward OAA synthesis and shutting off the malate valve that transports excess reductive equivalents to cytosol (Scheibe et al., 1986; Scheibe, 1987; Backhausen et al., 1994, 2000; Fig. 6). In addition, in C_3 plants, including poplar (*Populus* spp.), a NADP$^+$-dependent malic enzyme is present in chloroplasts (Van Doorsselaere et al., 1991; Lai et al., 2002; Yu et al., 2013), and accordingly, increased malic enzyme activity could also contribute to enhanced NADPH/NADP$^+$ unless the extra NADPH were fully used to support other chloroplastic processes (e.g. fatty acid synthesis; Fig. 6). In malate-fed rice leaves, an enhanced NADPH/NADP$^+$ ratio was observed (Cui et al., 2015), suggesting that the capacity of NADPH-consuming processes is not sufficient to fully consume the excess reductive equivalents.

Increased reductive pressure on the ferredoxin NADP$^+$ oxidoreductase can further lead to photoinhibition of PSI (Sonoike, 2011), ultimately feedback inhibiting the linear electron transport rate as observed in our study (Table I) and, likely, also the cyclic electron flow around PSI (Munekage et al., 2004; Johnson, 2011; Rochaix, 2011). Thus, we suggest that, in malate-fed leaves, overreduction of chloroplast stroma due to increased NADPH/NADP$^+$ ratio and imbalance between NADPH and ATP levels was responsible for the reduced rate of photosynthetic electron transport, further suppressing the rates of RuBP carboxylation and net assimilation (Table I). Given that chloroplastic malate dehydrogenase is activated by reduced thioredoxin (Schepens et al., 2000) that, in turn, gets electrons from reduced ferredoxin (Nikkanen and Rintamäki, 2014), a decrease in thioredoxin reductive status upon the inhibition of PSI electron transport is expected to lead to a decrease in malate dehydrogenase activity, thereby easing the reductive pressure. This can ultimately avoid progressive overreduction of electron carriers and lead to the stabilization of leaf photosynthetic rate at a new lower steady-state level, as observed in our study (Fig. 2).

The initial rise of stomatal conductance upon malate feeding (Fig. 2) is in accordance with the evidence that increases in guard cell malate concentrations lead to

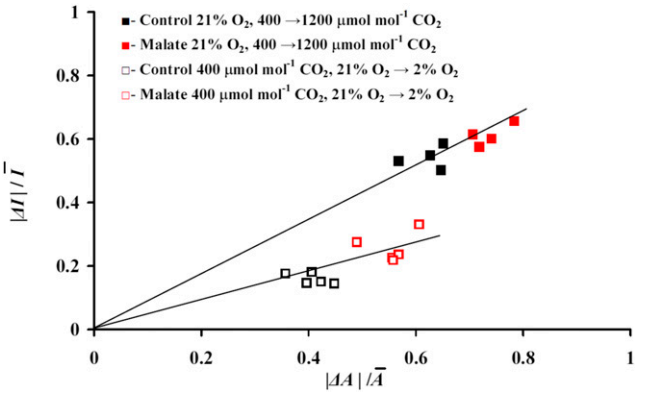

Figure 4. Correlations among relative changes in net assimilation rate ($R_{c,A} = \Delta A/\bar{A}$) and isoprene emission ($R_{c,I} = \Delta I/\bar{I}$) due to changes in ambient CO_2 concentration from 400 to 1,200 μmol mol^{-1} under 21% oxygen and due to changes in ambient oxygen concentration from 21% to 2% under 400 μmol mol^{-1} in control and malate-inhibited leaves across different experiments (for sample experiments, see Fig. 3). Here, ΔA and ΔI are differences in steady-state net assimilation and isoprene emission rates before and after the change in gas composition, and $\bar{A}$ and $\bar{I}$ are average values for these steady states (Rasulov et al., 2016). To show the data in the same scale, we used here the absolute differences $|\Delta A|$ and $|\Delta I|$ (for average nontransformed data, see Table III).

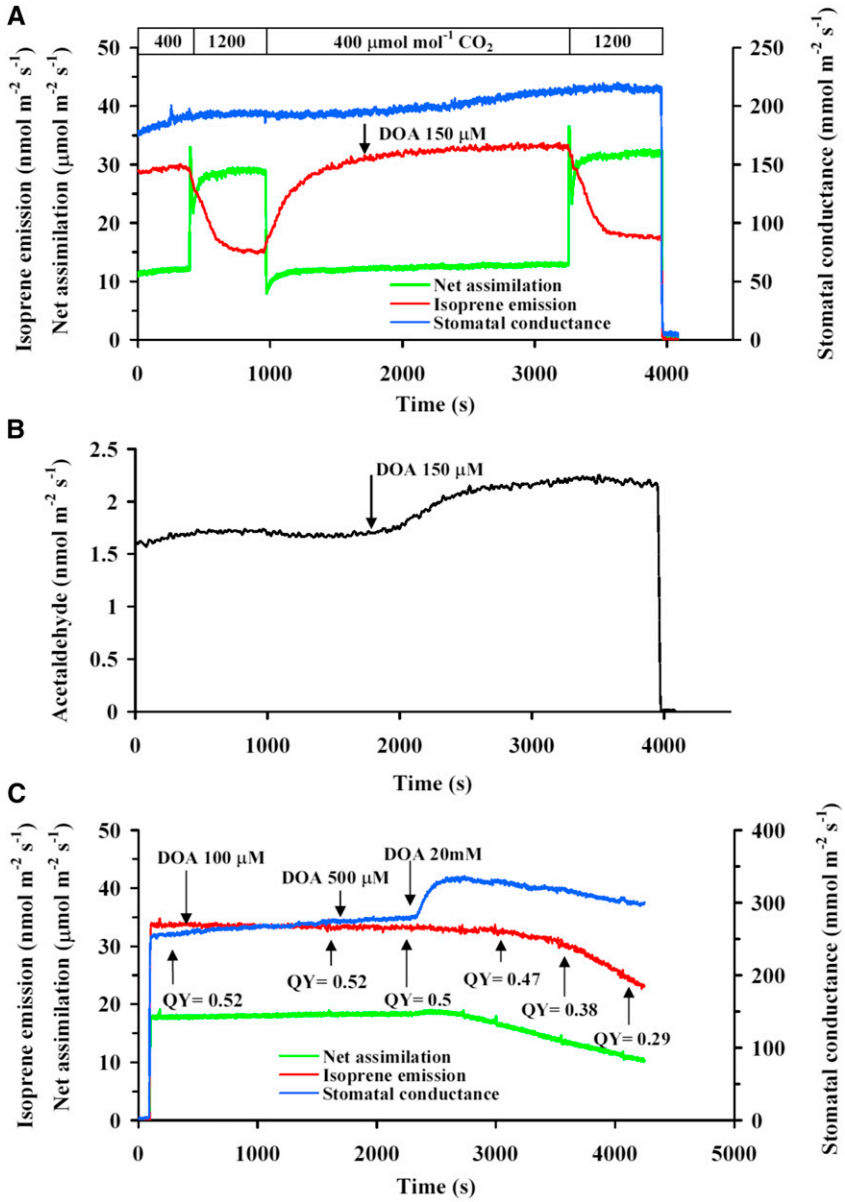

Figure 5. Characteristic responses of isoprene emission and net assimilation rates and stomatal conductance to changes in ambient CO_2 concentration (A) and acetaldehyde emission (B) in a hybrid aspen leaf before (0–1,800 s) and after (1,800–4,000 s) application of 150 μM of the specific PEPC inhibitor diethyl oxalacetate (DOA), and DOA dose response at ambient CO_2 concentration of 400 μmol mol^{-1} (C). Data presentation is as in Figure 3.

stomatal opening (Dittrich and Raschke, 1977; Travis and Mansfield, 1977). On the other hand, extracellular malate together with abscisic acid also activates so-called slow anion channels (S-type channels), inducing long-term stomatal closure (Esser et al., 1997), as observed in our study after the initial rise of stomatal openness (Fig. 2). Nevertheless, given that the C_i was reduced only moderately by malate feeding (Table I), we argue that the stomatal effects were complementary to biochemical down-regulation and not the primary cause of photosynthetic decline in malate-fed leaves. We note, however, that malate feeding could have resulted in a certain patchiness in stomatal openness, as is often observed in stressed leaves (Mott, 1995; Mott and Buckley, 1998). Such a patchiness could explain the greater changes in net assimilation rate to altered air composition in malate-fed leaves than could be expected on the basis of the moderate decrease of the C_i calculated assuming uniform stomatal openness (see below).

Malate Feeding in Relation to Respiratory Processes

In our study, malate feeding resulted in the enhancement of both dark respiration and photorespiration rates (Table I) that can have resulted from increased activity of multiple processes (Fig. 6). As malate is a key metabolite in the mitochondrial Krebs cycle, increased respiratory substrate availability can provide an explanation for the enhanced dark respiration rate. In fact, ^{14}C-labeling experiments have demonstrated that increases in malate concentration lead to increased citric acid concentration and the activation of mitochondrial

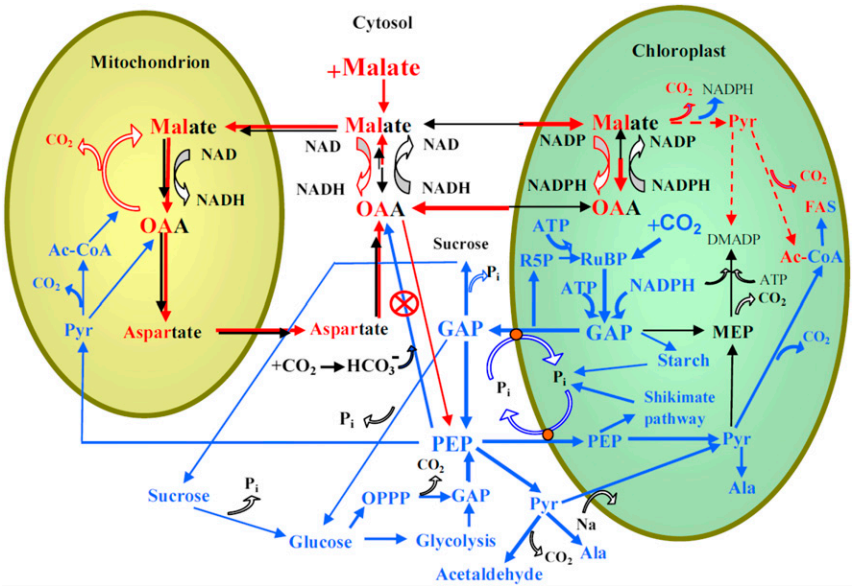

Figure 6. Postulated scheme of the relationships between cytosolic, chloroplastic, and mitochondrial processes as affected by exogenous feeding by malate and increases in CO_2 concentration. The processes enhanced by malate feeding are shown by red lines, whereas the thickness of the lines corresponds to the proposed magnitude of fluxes. Mixed red and black fonts denote compound pools affected by malate feeding. The processes suggested to be involved in the responses of photosynthesis and isoprene emission to the rise in CO_2 (Fig. 1) are shown by blue lines, and the corresponding compound pools are shown by blue font. The action of PEPC-specific inhibitors such as DOA used in our study (Fig. 5) is also shown. The key effect of exogenous malate is the reversal of the malate-OAA shuttle such that the chloroplast reductive status increases. This leads to feedback inhibition of photosynthetic electron transport, ultimately suppressing net assimilation (Table I) and isoprene emission rates due to curbed DMADP pool size (Table II). The cytosolic PEP pool size is determined by PEP formation from GAP, its export to chloroplasts and mitochondria, and carboxylation to OAA by PEPC. Cytosolic GAP can originate from chloroplasts or be formed via glycolysis or via the oxidative pentose phosphate cycle (OPPP). Malate accumulation in cytosol enhances OAA concentration, curbing PEPC activity and enhancing cytosolic PEP pool size and transport into chloroplast. The activation of $NADP^+$-malic enzyme in malate-fed leaves can further increase chloroplastic pyruvate (Pyr) concentrations, and cytosolic pyruvate can also be transported directly to chloroplast via an Na-dependent carrier (Furumoto et al., 2011). Enhanced dark and light respiration in malate-fed leaves is associated with both greater mitochondrial respiratory substrate availability and increased release of CO_2 due to chloroplastic processes positively affected by malate feeding, including increased malic enzyme activity and fatty acid synthesis. Malate-feeding (Table II; Fig. 3) and DOA-feeding (Fig. 4) experiments indicate that cytosolic PEP availability cannot curb isoprene emission under high CO_2 concentration, contrary to the hypothesis (Fig. 1). In fact, multiple pieces of evidence indicate that elevated CO_2 actually enhances chloroplastic pyruvate levels (Rasulov et al., 2009b, 2011). Instead, the experimental evidence in this study suggests that the elevated CO_2-dependent reduction in isoprene emission is due to the reduced share of photosynthetic electron flow to isoprene.

respiration both in the light and in the dark (Browse et al., 1980).

Given the reduction of net assimilation rate primarily due to nonstomatal processes in malate-fed leaves, the enhanced photorespiration rate is somewhat paradoxical, although C_i did drop somewhat, contributing to the greater photorespiration rate (Table I; see above for possible stomatal patchiness effects). However, as noted in "Materials and Methods," the experimental estimates of photorespiration in this study also include the component of mitochondrial respiration remaining in light as well as other nonphotorespiratory CO_2-releasing processes in light. Regarding these other CO_2-releasing processes activated by malate, the enhanced activity of C_3 plant $NADP^+$-malic enzyme that decarboxylates malate to pyruvate, releasing CO_2 (Van Doorsselaere et al., 1991; Lai et al., 2002; Yu et al., 2013), and the enhanced use of malate in fatty acid synthesis (Smith et al., 1992; Pleite et al., 2005) are possible candidates (Fig. 6). Overall, the respiration data further confirm that, in our study, malate did enter into primary metabolism and enhanc the rate of processes other than photosynthesis.

Inhibition of Isoprene Emission by Malate

There is evidence that malate inhibits PEPC both in C_4 (Wedding and Black, 1986) and in C_3 (Asai et al., 2000; Feria et al., 2008) plants. As hypothesized (Fig. 1), such an inhibition is expected to enhance cytosolic PEP concentration, thereby leading to greater transport of PEP into chloroplasts and use for the synthesis of DMADP in the MEP/DOXP pathway. Furthermore,

given that cytosolic malate and OAA are in equilibrium, an enhancement of cytosolic PEP pool size via increases in OAA decarboxylation under conditions of elevated malate is also possible (Fig. 6), as confirmed experimentally in Arabidopsis (*Arabidopsis thaliana*; Rylott et al., 2003).

Contrary to the hypothesis (Fig. 1), isoprene emission actually decreased in malate-fed leaves (Table II, Figs. 2 and 3A), whereas the kinetic characteristics of isoprene synthase, the maximum activity of isoprene synthase, and isoprene synthase rate constant were not affected and the apparent K_m of isoprene synthase was somewhat reduced by malate feeding (Table II). In fact, the reduction in isoprene emission in malate-fed leaves was associated primarily with reductions in DMADP pool size (Table II). On the other hand, the dark pool of MEP/DOXP pathway metabolites, consisting primarily of MEcDP (Li and Sharkey, 2013a, 2013b), was not affected significantly by malate feeding, but relative to DMADP pool size, it was much greater in malate-fed leaves (Table II). Thus, the overall MEP/DOXP pathway activity and isoprene synthase activity did not appear to be limiting, but it was mainly the conversion of MEcDP to DMADP that curbed the DMADP pool size and the rate of isoprene emission in malate-fed leaves. Given that reductions in isoprene emission rate and DMADP pool size were correlated strongly with changes in the effective quantum yield of PSII, this evidence suggests that it is the reduction in the activity of light reactions of photosynthesis that is responsible for decreases in isoprene emission, rather than the availability of carbon intermediates. As the conversion of MEcDP to DMADP requires two reductive steps, reductive limitation of DMADP pool size in malate-inhibited leaves seems to contradict the suggestion that malate enhanced the chloroplastic NADPH level (see above). However, in light, the two last reactions, catalyzed by HDS and HDR, directly consume electrons from reduced ferredoxin (Okada and Hase, 2005; Seemann et al., 2006; Rasulov et al., 2011; Banerjee and Sharkey, 2014), suggesting that malate-dependent changes in ferredoxin reductive status could have been primarily responsible for the observed inhibition of isoprene emission in malate-fed leaves. As discussed above, the reduction in whole-chain photosynthetic electron transport in malate-fed leaves (Table I) was likely initiated by suppression of the terminal steps of linear photosynthetic electron transport, in particular suppression of the activity of ferredoxin $NADP^+$ oxidoreductase, ultimately leading to the inhibition of PSI activity, including electron transfer to oxidized ferredoxin. Such a sequence of events is consistent with the limitation of isoprene emission in our study by the last two reductive steps.

Effects of Malate Inhibition on the Responses of Photosynthesis and Isoprene Emission to Increases in CO_2 under Normal Oxygen Concentration

We observed that increases in CO_2 concentration from 400 to 1,200 μmol mol^{-1} enhanced the rate of net assimilation and reduced the rate of isoprene emission in both control and malate-inhibited leaves (Fig. 3; Table III). This is the classical response of isoprene emission observed across numerous studies (see Introduction). Importantly, we did not find a significant effect of malate feeding on the sensitivity of isoprene emission to increases in CO_2 concentration (Table III), especially when the sensitivity was compared at a given change in net assimilation rate (Fig. 4). The increase in the rate of net assimilation upon the rise of CO_2 concentration was somewhat greater in malate-inhibited leaves, likely because of their lower stomatal conductance and greater photorespiration rate (Tables I and III; Fig. 3; see above for discussion of the effects of possible patchiness in stomatal openness in malate-fed leaves). Given that malate feeding and the concomitant enhanced levels of PEP and pyruvate did not abolish the high-CO_2-dependent reduction in isoprene emission, this evidence suggests that PEP and pyruvate availability did not limit isoprene emission under high CO_2 concentration.

Different from the PEP control hypothesis (Fig. 1), our data are consistent with the hypothesis that high-CO_2-dependent inhibition is due to a reduction in the share of photosynthetic electron flow going to isoprene synthesis (Rasulov et al., 2011, 2016). It is well known that, at high CO_2 concentration, the rate of net assimilation is limited by the regeneration of RuBP, either because of limited photosynthetic electron transport or the regeneration of inorganic phosphate (Sharkey, 1985, 1990; Dietz and Foyer, 1986; Sharkey and Vanderveer, 1989; Makino, 1994). Thus, under higher CO_2 concentration, the enhancement of net assimilation rate implies that a greater share of photosynthetic NADPH and ATP is used for photosynthesis, leading to both lower MEcDP and DMADP pools (Rasulov et al., 2011). Based on an analysis of the dynamics of isoprene emission under feedback-limited conditions, where oscillations in isoprene emission accompanying proportional oscillations in photosynthesis were associated with large MEcDP pools, it was concluded that it is ultimately the reductive equivalents that drive the observed competition between photosynthesis and isoprene emission (Rasulov et al., 2016). Given that malate feeding led to high MEcDP pools relative to DMADP pools, we conclude that the proposed mechanism of isoprene emission reduction by photosynthetic reductive equivalents (i.e. by the availability of reduced ferredoxin in the new inhibited steady state) is also operative in malate-fed leaves.

Differences in Oxygen Responses of Net Assimilation and Isoprene Emission Rates in Control and Malate-Fed Leaves

Under the ambient CO_2 concentration of 400 μmol mol^{-1}, the reduction of oxygen concentration from 21% to 2% increased the net assimilation rate and isoprene emission in both control and malate-fed leaves (Fig. 3; Table III). Again, the suppression of photorespiration

altered net assimilation rate in malate-fed leaves more than in control leaves (Table III) due to a greater photorespiration rate in malate-fed leaves (Table I). Analogous increases in isoprene emission in low oxygen under the ambient CO_2 have been shown in several studies (Monson and Fall, 1989; Loreto and Sharkey, 1993; Rasulov et al., 2009b, 2011). This is consistent with the mechanism of control of isoprene emission by photosynthetic light reactions; as the photorespiratory sink for ATP and reductive equivalents is reduced strongly under low oxygen, a greater share of electron flow is expected to go into isoprene synthesis (Rasulov et al., 2009b). It has been shown that the conditions of ambient CO_2 and low oxygen are associated with increases in both DMADP and MEcDP pool sizes (Rasulov et al., 2011; Li and Sharkey, 2013a), suggesting that both greater ATP and reductive equivalent availability explain the increased isoprene emission rate. Despite the overall suppression of isoprene emission and photosynthetic electron transport activities, the greater sensitivity of isoprene emission to low oxygen in malate-fed leaves (Table III) can be explained by their greater photorespiration rate, at least for the time window of the transition in oxygen concentration, approximately 400 s, used in our study (Fig. 3B). In addition, a suddenly enhanced availability of reduced ferredoxin can lead to an enhanced conversion of existing MEcDP pool to DMADP (Table II) and support the greater relative increase in isoprene emission rate in malate-fed leaves.

In contrast to the low-oxygen effects under the ambient CO_2 concentration, the reduction of oxygen concentration under high CO_2 concentration of 1,200 μmol mol^{-1} resulted in reductions in net assimilation rate and isoprene emission in both control and malate-fed leaves (Fig. 3). The negative oxygen response of photosynthesis suggests that, under high CO_2, photosynthesis became feedback limited (Sharkey, 1990). In particular, in control leaves, the transfer of leaves to low oxygen under high CO_2 was associated with oscillations in net assimilation rate and chlorophyll fluorescence (Fig. 3A; Supplemental Fig. S1), suggesting that photosynthesis was limited by the regeneration of triose phosphates due to low stromal phosphate levels that ultimately inhibited the rate of ATP formation and whole-chain linear electron transport (Sharkey, 1990; Pammenter et al., 1993). In control leaves, oscillations in net assimilation rate were also accompanied by oscillations in isoprene emission, although to a lower extent (Fig. 3A; Supplemental Fig. S1). As demonstrated experimentally by Rasulov et al. (2016), the lower amplitude of oscillations in isoprene emission than in net assimilation rate is due to the buffering of changes in isoprene synthesis rate by existing pools of MEcDP and DMADP. Nonetheless, the oscillations in isoprene emission do indicate that, in the control leaves, the reduction in electron transport rate did limit the isoprene emission of control leaves under low oxygen and high CO_2.

Different from control leaves, photosynthetic oscillations were absent or heavily suppressed in malate-fed leaves under low oxygen and high CO_2 (Fig. 3B), but the reduction in net assimilation rate was relatively greater and the reduction in isoprene emission rate was smaller in malate-fed leaves (Table III). The overall stronger inhibition of net assimilation rate suggests a stronger feedback limitation in malate-fed leaves, but the lack of oscillations is puzzling. However, given the strongly suppressed photosynthetic electron transport rate already prior to the change in oxygen concentration (Fig. 3B; Table I), the lack of oscillations might be indicative of lower levels and lower fluctuations in ATP and RuBP pool sizes in the background of a high NADPH level. On the other hand, given the greater MEcDP pool size in malate-fed leaves, ATP was less limiting for isoprene emission than for photosynthesis. Thus, due to the stronger photosynthetic suppression as the result of low ATP level, the last reductive steps in the MEP/DOXP pathway likely had temporarily greater access to reduced ferredoxin, explaining the lower suppression of the isoprene emission rate.

This evidence has important implications for the hypothesis of the limitation of isoprene emission by cytosolic PEP. PEP transport from the cytosol into chloroplasts by PEP/phosphate translocator is bound to the stoichiometric antiport of phosphate (Flügge et al., 2011). Thus, in feedback-inhibited conditions, when the chloroplastic phosphate level is low, PEP transport into the chloroplasts could be limited by chloroplastic phosphate availability (Li and Sharkey, 2013b; Banerjee and Sharkey, 2014). While malate feeding must have enhanced the PEP level, the feedback inhibition was actually more severe in malate-fed leaves, and the somewhat lower reduction in isoprene emission rate under these conditions (Table III) is not consistent with the PEP/phosphate antiport limitation hypothesis.

Limited Effect of DOA on Photosynthesis and Isoprene Emission

To further test the hypothesis of the role of cytosolic PEPC in isoprene synthesis (Fig. 1), we used the specific PEPC inhibitor DOA (Walker and Edwards, 1990; Magnin et al., 1997). Initially, we used 150 μM DOA, similar to previous studies (Magnin et al., 1997; Rosenstiel et al., 2003). However, we did not observe any effect of DOA applied at this concentration on foliage photosynthesis and isoprene emission rates (Fig. 5A), and contrary to our expectations, isoprene emission rate actually even decreased at the highest DOA concentration applied (Fig. 5C). Lack of an effect on photosynthesis is consistent with the study of Walker and Edwards (1990), who did also not observe changes in foliage photosynthesis in DOA-treated C_3 plants. More importantly, we did not observe any change in the high-CO_2 response of isoprene emission in DOA-fed leaves (Fig. 5A). Our data are in contrast to an experiment with a poplar leaf by Rosenstiel et al. (2003), where an approximately 25% increase of isoprene emission in 10 min after the application of 100 μM DOA was observed, and this increase was also associated with an

approximately 10% reduction in net assimilation rate. We cannot explain this discrepancy with our experiments, but we note that the data of Rosenstiel et al. (2003) are of lower resolution (10-min resolution) and lack the essential supporting information, such as stomatal conductance and photosynthetic electron transport rate.

On the other hand, the application of 150 μM DOA resulted in an enhancement of acetaldehyde emission (Fig. 5B). This is consistent with the pyruvate-overflow mechanism (Karl et al., 2002) and indicates that cytosolic PEP level was indeed enhanced by DOA feeding in our study. Altogether, the DOA experiments in our study further support the evidence from malate-feeding experiments that the cytosolic PEP level does not limit leaf isoprene emissions under both low and high CO_2 concentrations.

CONCLUSION

The malate- and DOA-feeding experiments carried out in this study suggested that the availability of chloroplastic PEP level is not responsible for the reduction in isoprene emission under high CO_2 concentration. In particular, the inhibition of PEPC activity that has been assumed to lead to the suppression of isoprene emission under high CO_2 (Fig. 1) did not relieve the CO_2 limitation of isoprene emission (Table III). The primary effect of malate feeding was the alteration of leaf reductive status, with different modifications in net assimilation rate and isoprene emission as a result of the suppression of photosynthetic electron transport and the changed balance between ATP, NADPH, and reduced ferredoxin. Overall, the experimental data were consistent with the understanding that high CO_2 reduces isoprene emission due to a lower share of reductive and energetic equivalents available for isoprene emission, whereas the primary limiting steps in the MEP/DOXP pathway are the reductive reactions converting MEcDP to DMADP, in particular the last two reactions catalyzed by HDS and HDR that accept electrons directly from reduced ferredoxin in the photosynthetic electron transport chain. Across different CO_2 and oxygen concentrations, the photosynthetic use of photosynthetic electron flow was prioritized, whereas the magnitude of changes in isoprene emission after the modification of air composition was dependent on the degree of limitation of photosynthesis by photosynthetic electron transport. We suggest that the RuBP pool is the key sink of photosynthetic electron flow that determines the concentrations of ATP and reductive equivalents available for isoprene emission. Increases in CO_2 concentration under normal oxygen that reduced RuBP pool size (Badger et al., 1984; Laisk et al., 2002; Rasulov et al., 2016) and increased net assimilation rate resulted in lower isoprene emission rate, while decreases of oxygen concentration under ambient CO_2 that increased RuBP pool size (Badger et al., 1984; Laisk et al., 2002; Rasulov et al., 2016) and enhanced photosynthesis increased isoprene emission rate. In the case of feedback-limited conditions, under high CO_2 and low oxygen and low RuBP pool (Sharkey, 1990; Laisk et al., 2002; Rasulov et al., 2016), both photosynthesis and isoprene emission were reduced. Although the absolute drain of photosynthetic electron flow to isoprene synthesis is small, such a regulation of isoprene emission is plausible, provided that the effective Michaelis-Menten constant of the MEP/DOXP pathway for ATP and reductive equivalents is high (i.e. isoprene emission does not compete directly with photosynthetic carbon assimilation for electron flow but tracks the leaf energetic and reductive status).

MATERIALS AND METHODS

Plant Material and Growth Conditions

We used 2-year-old plants of hybrid aspen (*Populus tremula* × *Populus tremuloides* clone H200) as in our previous studies on environmental controls of isoprene emission (Rasulov et al., 2009a, 2011, 2015b). The saplings were planted in 4-L pots filled with a blend of commercial planting soil and sand (1:1) with slow-release balanced fertilizer and grown in a Fitoclima S600 PLLH growth chamber (Aralab). The photosynthetically active quantum flux density at plant level was kept at 700 μmol m^{-2} s^{-1} for a 14-h day, day/night temperatures were 25°C/22°C, relative air humidity at daytime was 60%, and ambient CO_2 concentration was 400 μmol mol^{-1}. For optimum water supply, the saplings were watered to soil field capacity every other day. The experiments were conducted with fully expanded 20- to 25-d-old leaves that had peak-level net assimilation and isoprene emission rates (for ontogenetic changes in leaf physiological capacities in aspen, see Rasulov et al., 2014).

Leaf Malate-Feeding Treatments

Excised leaves were fed through the petiole with malate (Sigma-Aldrich) solution or with distilled water (control). A malate concentration of 20 mM was used in these experiments (the inhibitory constant of PEPC for malate is approximately 4–8 mM; Huber and Sugiyama, 1986; Wedding et al., 1990; Gupta et al., 1994; Parvathi et al., 2000). After leaf excision, the petiole was kept in a 2-mL vial filled with distilled water until leaf gas-exchange rates and isoprene emissions reached a maximum value at standard measurement conditions (see below), typically for 20 min after leaf excision. Malate treatment was started by rapidly withdrawing 1 mL of the distilled water by one syringe while simultaneously adding 1 mL of 40 mM malate solution with another syringe, such that the desired malate concentration was achieved almost immediately while avoiding exposure of the cut end of the petiole to ambient air. The control leaves were maintained in distilled water through the experiments.

Inhibition of the PEPC Reaction by diethyl oxalacetate (DOA)

To inhibit PEPC activity, the leaves were fed with DOA (Sigma-Aldrich) analogously as in malate treatments. We initially used the concentration of 150 μM, similar to that employed in previous studies (Magnin et al., 1997; Rosenstiel et al., 2003), in agreement with the reported low PEPC inhibitory constant for DOA of 4 to 9 μM (Walker et al., 1986; Walker and Edwards, 1990). In addition, higher concentrations of 500 μM and 20 mM were also used.

Measurements of Foliage Gas-Exchange Rates, Isoprene Emission, and Chlorophyll Fluorescence

We used an ultrafast-response (system half-time of approximately 0.15 s for a stepwise change in chamber gas concentration), two-channel, custom-made gas-exchange system specially designed for measurements of rapid transients in foliage gas-exchange rates after changes in ambient conditions (Rasulov et al., 2011, 2015b). For rapid changes in air CO_2 and oxygen concentrations in the leaf chamber, different air compositions can be prepared separately in the reference and measurement lines, and upon switching the gas lines by solenoid valves (ASCO SC precision solenoid valves; ASCO Valves), the gas concentrations in the measurement channel can be changed almost instantaneously.

To measure gas concentrations in the air going into and exiting the leaf chamber, an LI-6251 infrared gas analyzer (LI-COR) was used for CO_2, a custom-made psychrometer for water vapor, and an N-22M Ametek oxygen analyzer (Ametek) for oxygen concentration measurements (Rasulov et al., 2009a). In most experiments, isoprene concentration was measured by a proton-transfer reaction quadrupole mass-spectrometer (PTR-QMS; a high-sensitivity version with a response time of approximately 0.1 s; Ionicon Analytik). In experiments with DOA inhibition, a proton-transfer reaction time-of-flight mass-spectrometer (PTR-TOF-MS 8000; Ionicon Analytik) was used. The operation of PTR-QMS was as in our previous studies (Rasulov et al., 2014, 2015b, 2016), while the operation of the PTR-TOF-MS followed the protocol of Portillo-Estrada et al. (2015). Isoprene was detected as the protonated parent ion with mass-to-charge ratio of 69^+ in PTR-QMS measurements (Graus et al., 2004; Rasulov et al., 2014) and of 69.07^+ in PTR-TOF-MS measurements (Brilli et al., 2011; Portillo-Estrada et al., 2015). In addition, acetaldehyde (mass-to-charge ratio of 44.054^+) was analyzed in DOA inhibition experiments. A calibration gas containing representatives of key plant volatile classes, including isoprene and acetaldehyde (Ionimed), was employed to calibrate both PTR-QMS and PTR-TOF-MS instruments.

Steady-state (F) and maximum (F_m') light-adapted fluorescence yields were measured with a pulse amplitude-modulated chlorophyll fluorimeter (PAM 101; Walz). The measurement light was modulated at 100 kHz, and the white light intensity during saturated pulses (1 s) of light for F_m' determination was 10,000 μmol m^{-2} s^{-1} (Rasulov et al., 2009b). In addition, an estimate of minimum fluorescence yield in a partly relaxed state in light ($F_{0,a}$) was made by illuminating the leaves with far-red light (150 μmol m^{-2} s^{-1}).

Protocol for Physiological Measurements and Derivation of Key Gas-Exchange and Isoprene Emission Characteristics

After enclosure of the leaf in the gas-exchange cuvette, the leaf was stabilized under standard conditions (ambient CO_2 concentration of 400 μmol mol^{-1}, oxygen concentration of 21% (v/v), relative air humidity of 60% (v/v), leaf temperature of 30°C, and saturating light intensity of 700 μmol m^{-2} s^{-1}) until stomata fully opened and net assimilation and isoprene emission rates reached steady-state values, typically 20 min after leaf enclosure. Once the steady-state values had been reached, leaf chamber CO_2 and/or oxygen concentrations were changed rapidly to induce conditions of feedback-limited photosynthesis and decreased reductant supply (high CO_2 concentration, low oxygen concentration, or low oxygen and high CO_2 concentrations; Rasulov et al., 2016).

In steady-state conditions, the pool size of the immediate isoprene precursor (DMADP, and part of isopentenyl diphosphate) and the pool size of upstream metabolites (dark pool; the pool of MEP/DOXP pathway intermediates prior to the HDS and HDR reactions, mainly MEcDP) were estimated from the postillumination kinetics of isoprene emission (Rasulov et al., 2009a, 2011; Li et al., 2011; Weise et al., 2013). The DMADP pool size supporting the given rate of isoprene emission in light corresponds to the integral of the rapid decay of isoprene emission after switching off the light, for approximately 200 to 250 s after the darkening. In the dark, a second rise of isoprene emission occurs between approximately 250 and 600 s, and the integral of this second emission release provides the size of the dark pool (Rasulov et al., 2009a, 2011; Li et al., 2011).

From the rapid dark decay kinetics, paired values of DMADP pool size remaining at the given moment of time and isoprene emission rate corresponding to the given DMADP pool size were derived and used to determine the in vivo values of the K_m (nmol m^{-2}) and V_{max} (nmol m^{-2} s^{-1}) of isoprene synthase using the Hanes-Woolf plot (Rasulov et al., 2009a, 2011). These data were also used to estimate the initial slope of isoprene emission versus DMADP pool size dependency (isoprene synthase rate constant).

Calculations of foliage net assimilation rate (A), stomatal conductance to water vapor, and intercellular CO2 concentration (C_i) followed von Caemmerer and Farquhar (1981). The apparent V_{cmax} was estimated from the initial slope of the A versus C_i response curve according to Niinemets et al. (1999a) using the kinetic characteristics of Rubisco of Jordan and Ogren (1984). The rate of photorespiration was estimated by two approaches. First, the air without CO_2 was used to measure the rate of leaf CO_2 release immediately after switching to CO_2-free air (Keys et al., 1977). The second estimate of photorespiration was obtained from the rate of postillumination CO_2 burst immediately after leaf darkening; under these transient conditions, the leaf CO_2 release is dependent primarily on the rate of photorespiration (Peterson, 1983). Both measurements gave similar values, but we note that there is a certain bias with both estimates because they also include a component of mitochondrial respiration remaining in light. In addition, the estimate based on postillumination CO_2 burst also includes CO_2 uptake due to the consumption of RuBP formed in light (Sharkey, 1988; Farquhar and Busch, 2017). The rate of dark respiration was recorded after the dark CO_2 release had reached a steady state, typically after 5 to 10 min of leaf darkening. The light-adapted quantum yield of PSII was estimated from chlorophyll fluorescence characteristics as $QY = (F_m' - F)/F_m'$ (Genty et al., 1989).

For the experiments with changing CO_2 and oxygen concentrations, we calculated both relative changes in net assimilation rate ($R_{c,A}$) and isoprene emission rate ($R_{c,I}$) for different steady-state situations. For net assimilation, $R_{c,A} = \Delta A/\bar{A}$, where ΔA is the difference in net assimilation rate between the two steady-state values and $\bar{A}$ is the average value obtained for the two steady-state conditions (Rasulov et al., 2016). The relative change for isoprene emission was calculated analogously.

All experiments were replicated four to five times with different leaves, and means ± SE of all photosynthetic and isoprene emission characteristics were estimated in the steady state (Tables I and II).

Supplemental Data

The following supplemental materials are available.

Supplemental Figure S1. Changes in isoprene emission and net assimilation rates and stomatal conductance in response to modifications in atmospheric CO_2 and oxygen concentrations.

Received October 6, 2017; accepted December 8, 2017; published December 12, 2017.

LITERATURE CITED

Asai N, Nakajima N, Tamaoki M, Kamada H, Kondo N (2000) Role of malate synthesis mediated by phosphoenolpyruvate carboxylase in guard cells in the regulation of stomatal movement. Plant Cell Physiol **41:** 10–15

Backhausen JE, Kitzmann C, Horton P, Scheibe R (2000) Electron acceptors in isolated intact spinach chloroplasts act hierarchically to prevent over-reduction and competition for electrons. Photosynth Res **64:** 1–13

Backhausen JE, Kitzmann C, Scheibe R (1994) Competition between electron acceptors in photosynthesis: regulation of the malate valve during CO_2 fixation and nitrite reduction. Photosynth Res **42:** 75–86

Badger MR, Sharkey TD, von Caemmerer S (1984) The relationship between steady-state gas exchange of bean leaves and the levels of carbon-reduction-cycle intermediates. Planta **160:** 305–313

Banerjee A, Sharkey TD (2014) Methylerythritol 4-phosphate (MEP) pathway metabolic regulation. Nat Prod Rep **31:** 1043–1055

Brilli F, Ruuskanen TM, Schnitzhofer R, Müller M, Breitenlechner M, Bittner V, Wohlfahrt G, Loreto F, Hansel A (2011) Detection of plant volatiles after leaf wounding and darkening by proton transfer reaction "time-of-flight" mass spectrometry (PTR-TOF). PLoS ONE **6:** e20419

Browse JA, Brown JMA, Dromgoole FI (1980) Malate synthesis and metabolism during photosynthesis in *Egeria densa* Planch. Aquat Bot **8:** 295–305

Chinthapalli B, Murmu J, Raghavendra AS (2003) Dramatic difference in the responses of phosphoenolpyruvate carboxylase to temperature in leaves of C_3 and C_4 plants. J Exp Bot **54:** 707–714

Cui Z, Nian Y, Zhang A, Zang J, Zhu Y, Ruan Y, Fan J, Zhang L (2015) Exogenous malate application inhibits the photochemical activity of photosystem II in rice leaves. Int J Agric Biol **17:** 1265–1269

Delwiche CF, Sharkey TD (1993) Rapid appearance of ^{13}C in biogenic isoprene when $^{13}CO_2$ is fed to intact leaves. Plant Cell Environ **16:** 587–591

Dietz KJ, Foyer C (1986) The relationship between phosphate status and photosynthesis in leaves: reversibility of the effects of phosphate deficiency on photosynthesis. Planta **167:** 376–381

Dietz KJ, Neimanis S, Heber U (1984) Rate-limiting factors in leaf photosynthesis. I. Electron transport. Biochim Biophys Acta **767:** 444–450

Dittrich P, Raschke K (1977) Malate metabolism in isolated epidermis of *Commelina communis* L. in relation to stomatal functioning. Planta **134:** 77–81

Esser JE, Liao YJ, Schroeder JI (1997) Characterization of ion channel modulator effects on ABA- and malate-induced stomatal movements: strong regulation by kinase and phosphatase inhibitors, and relative insensitivity to mastoparans. J Exp Bot **48:** 539–550

Farquhar GD, Busch FA (2017) Changes in the chloroplastic CO_2 concentration explain much of the observed Kok effect: a model. New Phytol **214:** 570–584

Farquhar GD, von Caemmerer S, Berry JA (1980) A biochemical model of photosynthetic CO_2 assimilation in leaves of C_3 species. Planta **149:** 78–90

Feria AB, Alvarez R, Cochereau L, Vidal J, García-Mauriño S, Echevarría C (2008) Regulation of phosphoenolpyruvate carboxylase phosphorylation by metabolites and abscisic acid during the development and germination of barley seeds. Plant Physiol **148:** 761–774

Flügge UI, Häusler RE, Ludewig F, Gierth M (2011) The role of transporters in supplying energy to plant plastids. J Exp Bot **62:** 2381–2392

Furumoto T, Yamaguchi T, Ohshima-Ichie Y, Nakamura M, Tsuchida-Iwata Y, Shimamura M, Ohnishi J, Hata S, Gowik U, Westhoff P, et al (2011) A plastidial sodium-dependent pyruvate transporter. Nature **476:** 472–475

Genty B, Briantais JM, Baker NR (1989) The relationship between the quantum yield of photosynthetic electron transport and quenching of chlorophyll fluorescence. Biochim Biophys Acta **990:** 87–92

Ghirardo A, Wright LP, Bi Z, Rosenkranz M, Pulido P, Rodríguez-Concepción M, Niinemets Ü, Brüggemann N, Gershenzon J, Schnitzler JP (2014) Metabolic flux analysis of plastidic isoprenoid biosynthesis in poplar leaves emitting and nonemitting isoprene. Plant Physiol **165:** 37–51

Graus M, Schnitzler JP, Hansel A, Cojocariu C, Rennenberg H, Wisthaler A, Kreuzwieser J (2004) Transient release of oxygenated volatile organic compounds during light-dark transitions in grey poplar leaves. Plant Physiol **135:** 1967–1975

Grote R, Monson RK, Niinemets Ü (2013) Leaf-level models of constitutive and stress-driven volatile organic compound emissions. *In* Ü Niinemets, RK Monson, eds, Biology, Controls and Models of Tree Volatile Organic Compound Emissions. Springer, Berlin, pp 315–355

Guenther A (2013) Biological and chemical diversity of biogenic volatile organic emissions into the atmosphere. ISRN Atmospheric Sciences **2013:** 786290

Guenther AB, Jiang X, Heald CL, Sakulyanontvittaya T, Duhl T, Emmons LK, Wang X (2012) The Model of Emissions of Gases and Aerosols from Nature version 2.1 (MEGAN2.1): an extended and updated framework for modeling biogenic emissions. Geosci Model Dev **5:** 1471–1492

Gupta SK, Ku MSB, Lin JH, Zhang D, Edwards GE (1994) Light/dark modulation of phospho*enol*pyruvate carboxylase in C_3 and C_4 species. Photosynth Res **42:** 133–143

Heber U, Neimanis S, Dietz KJ, Viil J (1986) Assimilatory power as a driving force in photosynthesis. Biochim Biophys Acta **852:** 144–155

Huber SC, Sugiyama T (1986) Changes in sensitivity to effectors of maize leaf phosphoenolpyruvate carboxylase during light/dark transitions. Plant Physiol **81:** 674–677

Johnson GN (2011) Physiology of PSI cyclic electron transport in higher plants. Biochim Biophys Acta **1807:** 906–911

Jordan DB, Ogren WL (1984) The CO_2/O_2 specificity of ribulose 1,5-bisphosphate carboxylase/oxygenase: dependence on ribulosebisphosphate concentration, pH and temperature. Planta **161:** 308–313

Karl T, Curtis AJ, Rosenstiel TN, Monson RK, Fall R (2002) Transient releases of acetaldehyde from tree leaves: products of a pyruvate overflow mechanism. Plant Cell Environ **25:** 1121–1131

Keys AJ, Sampaio EVSB, Cornelius MJ, Bird IF (1977) Effect of temperature on photosynthesis and photorespiration of wheat leaves. J Exp Bot **28:** 525–533

Lai LB, Wang L, Nelson TM (2002) Distinct but conserved functions for two chloroplastic NADP-malic enzyme isoforms in C3 and C4 *Flaveria* species. Plant Physiol **128:** 125–139

Laisk A, Oja V, Rasulov B, Rämma H, Eichelmann H, Kasparova I, Pettai H, Padu E, Vapaavuori E (2002) A computer-operated routine of gas exchange and optical measurements to diagnose photosynthetic apparatus in leaves. Plant Cell Environ **25:** 923–943

Li Z, Ratliff EA, Sharkey TD (2011) Effect of temperature on postillumination isoprene emission in oak and poplar. Plant Physiol **155:** 1037–1046

Li Z, Sharkey TD (2013a) Metabolic profiling of the methylerythritol phosphate pathway reveals the source of post-illumination isoprene burst from leaves. Plant Cell Environ **36:** 429–437

Li Z, Sharkey TD (2013b) Molecular and pathway controls on biogenic volatile organic compound emissions. *In* Ü Niinemets, RK Monson, eds, Biology, Controls and Models of Tree Volatile Organic Compound Emissions. Springer, Berlin, pp 119–151

Loreto F, Sharkey TD (1990) A gas-exchange study of photosynthesis and isoprene emission in *Quercus rubra* L. Planta **182:** 523–531

Loreto F, Sharkey TD (1993) On the relationship between isoprene emission and photosynthetic metabolites under different environmental conditions. Planta **189:** 420–424

Magnin NC, Cooley BA, Reiskind JB, Bowes G (1997) Regulation and localization of key enzymes during the induction of Kranz-less, C_4-type photosynthesis in *Hydrilla verticillata*. Plant Physiol **115:** 1681–1689

Makino A (1994) Biochemistry of C_3-photosynthesis in high CO_2. J Plant Res **107:** 79–84

Monson RK, Fall R (1989) Isoprene emission from aspen leaves: influence of environment and relation to photosynthesis and photorespiration. Plant Physiol **90:** 267–274

Monson RK, Grote R, Niinemets Ü, Schnitzler JP (2012) Modeling the isoprene emission rate from leaves. New Phytol **195:** 541–559

Moraes TF, Plaxton WC (2000) Purification and characterization of phosphoenolpyruvate carboxylase from *Brassica napus* (rapeseed) suspension cell cultures: implications for phosphoenolpyruvate carboxylase regulation during phosphate starvation, and the integration of glycolysis with nitrogen assimilation. Eur J Biochem **267:** 4465–4476

Mott KA (1995) Effects of patchy stomatal closure on gas exchange measurements following abscisic acid treatment. Plant Cell Environ **18:** 1291–1300

Mott KA, Buckley TN (1998) Stomatal heterogeneity. J Exp Bot **49:** 407–417

Munekage Y, Hashimoto M, Miyake C, Tomizawa K, Endo T, Tasaka M, Shikanai T (2004) Cyclic electron flow around photosystem I is essential for photosynthesis. Nature **429:** 579–582

Niinemets Ü, Tenhunen JD, Canta NR, Chaves MM, Faria T, Pereira JS, Reynolds JF (1999a) Interactive effects of nitrogen and phosphorus on the acclimation potential of foliage photosynthetic properties of cork oak, *Quercus suber*, to elevated atmospheric CO_2 concentrations. Glob Change Biol **5:** 455–470

Niinemets Ü, Tenhunen JD, Harley PC, Steinbrecher R (1999b) A model of isoprene emission based on energetic requirements for isoprene synthesis and leaf photosynthetic properties for *Liquidambar* and *Quercus*. Plant Cell Environ **22:** 1319–1336

Nikkanen L, Rintamäki E (2014) Thioredoxin-dependent regulatory networks in chloroplasts under fluctuating light conditions. Philos Trans R Soc Lond B Biol Sci **369:** 20130224

Okada K, Hase T (2005) Cyanobacterial non-mevalonate pathway: (*E*)-4-hydroxy-3-methylbut-2-enyl diphosphate synthase interacts with ferredoxin in *Thermosynechococcus elongatus* BP-1. J Biol Chem **280:** 20672–20679

Pammenter NW, Loreto F, Sharkey TD (1993) End product feedback effects on photosynthetic electron transport. Photosynth Res **35:** 5–14

Parvathi K, Bhagwat AS, Ueno Y, Izui K, Raghavendra AS (2000) Illumination increases the affinity of phosphoenolpyruvate carboxylase to bicarbonate in leaves of a C_4 plant, *Amaranthus hypochondriacus*. Plant Cell Physiol **41:** 905–910

Peterson RB (1983) Estimation of photorespiration based on the initial rate of postillumination CO_2 release. I. A nonsteady state model for measurement of CO_2 exchange transients. Plant Physiol **73:** 978–982

Pleite R, Pike MJ, Garcés R, Martínez-Force E, Rawsthorne S (2005) The sources of carbon and reducing power for fatty acid synthesis in the heterotrophic plastids of developing sunflower (*Helianthus annuus* L.) embryos. J Exp Bot **56:** 1297–1303

Portillo-Estrada M, Kazantsev T, Talts E, Tosens T, Niinemets Ü (2015) Emission timetable and quantitative patterns of wound-induced volatiles across different damage treatments in aspen (*Populus tremula*). J Chem Ecol **41:** 1105–1117

Potosnak MJ (2014) Including the interactive effect of elevated CO_2 concentration and leaf temperature in global models of isoprene emission. Plant Cell Environ **37:** 1723–1726

Rasulov B, Bichele I, Hüve K, Vislap V, Niinemets Ü (2015a) Acclimation of isoprene emission and photosynthesis to growth temperature in hybrid aspen: resolving structural and physiological controls. Plant Cell Environ **38:** 751–766

Rasulov B, Bichele I, Laisk A, Niinemets Ü (2014) Competition between isoprene emission and pigment synthesis during leaf development in aspen. Plant Cell Environ **37:** 724–741

Rasulov B, Copolovici L, Laisk A, Niinemets Ü (2009a) Postillumination isoprene emission: in vivo measurements of dimethylallyldiphosphate

pool size and isoprene synthase kinetics in aspen leaves. Plant Physiol **149:** 1609–1618

Rasulov B, Hüve K, Laisk A, Niinemets Ü (2011) Induction of a longer term component of isoprene release in darkened aspen leaves: origin and regulation under different environmental conditions. Plant Physiol **156:** 816–831

Rasulov B, Hüve K, Välbe M, Laisk A, Niinemets Ü (2009b) Evidence that light, carbon dioxide, and oxygen dependencies of leaf isoprene emission are driven by energy status in hybrid aspen. Plant Physiol **151:** 448–460

Rasulov B, Talts E, Kännaste A, Niinemets Ü (2015b) Bisphosphonate inhibitors reveal a large elasticity of plastidic isoprenoid synthesis pathway in isoprene-emitting hybrid aspen. Plant Physiol **168:** 532–548

Rasulov B, Talts E, Niinemets Ü (2016) Spectacular oscillations in plant isoprene emission under transient conditions explain the enigmatic CO_2 response. Plant Physiol **172:** 2275–2285

Rochaix JD (2011) Regulation of photosynthetic electron transport. Biochim Biophys Acta **1807:** 375–383

Rosenstiel TN, Potosnak MJ, Griffin KL, Fall R, Monson RK (2003) Increased CO_2 uncouples growth from isoprene emission in an agriforest ecosystem. Nature **421:** 256–259

Rylott EL, Gilday AD, Graham IA (2003) The gluconeogenic enzyme phosphoenolpyruvate carboxykinase in *Arabidopsis* is essential for seedling establishment. Plant Physiol **131:** 1834–1842

Scheibe R (1987) $NADP^+$-malate dehydrogenase in C_3-plants: regulation and role of a light-activated enzyme. Physiol Plant **71:** 393–400

Scheibe R, Wagenpfeil D, Fischer J (1986) NADP-malate dehydrogenase activity during photosynthesis in illuminated spinach chloroplasts. Plant Physiol **124:** 103–110

Schepens I, Johansson K, Decottignies P, Gillibert M, Hirasawa M, Knaff DB, Miginiac-Maslow M (2000) Inhibition of the thioredoxin-dependent activation of the NADP-malate dehydrogenase and cofactor specificity. J Biol Chem **275:** 20996–21001

Seemann M, Tse Sum Bui B, Wolff M, Miginiac-Maslow M, Rohmer M (2006) Isoprenoid biosynthesis in plant chloroplasts via the MEP pathway: direct thylakoid/ferredoxin-dependent photoreduction of GcpE/IspG. FEBS Lett **580:** 1547–1552

Sharkey TD (1985) Photosynthesis in intact leaves of C_3 plants: physics, physiology and rate limitations. Bot Rev **51:** 53–105

Sharkey TD (1988) Estimating the rate of photorespiration in leaves. Physiol Plant **73:** 147–152

Sharkey TD (1990) Feedback limitation of photosynthesis and the physiological role of ribulose bisphosphate carboxylase carbamylation. Bot Mag Tokyo **2:** 87–105

Sharkey TD, Vanderveer PJ (1989) Stromal phosphate concentration is low during feedback limited photosynthesis. Plant Physiol **91:** 679–684

Sharkey TD, Weise SE (2016) The glucose 6-phosphate shunt around the Calvin-Benson cycle. J Exp Bot **67:** 4067–4077

Sharkey TD, Wiberley AE, Donohue AR (2008) Isoprene emission from plants: why and how. Ann Bot **101:** 5–18

Smith RG, Gauthier DA, Dennis DT, Turpin DH (1992) Malate- and pyruvate-dependent fatty acid synthesis in leucoplasts from developing castor endosperm. Plant Physiol **98:** 1233–1238

Sonoike K (2011) Photoinhibition of photosystem I. Physiol Plant **142:** 56–64

Travis AJ, Mansfield TA (1977) Studies of malate formation in isolated guard cells. New Phytol **78:** 541–546

Trowbridge AM, Asensio D, Eller ASD, Way DA, Wilkinson MJ, Schnitzler JP, Jackson RB, Monson RK (2012) Contribution of various carbon sources toward isoprene biosynthesis in poplar leaves mediated by altered atmospheric CO_2 concentrations. PLoS ONE **7:** e32387

Van Doorsselaere J, Villarroel R, Van Montagu M, Inzé D (1991) Nucleotide sequence of a cDNA encoding malic enzyme from poplar. Plant Physiol **96:** 1385–1386

von Caemmerer S (2000) Biochemical Models of Leaf Photosynthesis. CSIRO Publishing, Collingwood, Australia

von Caemmerer S, Farquhar GD (1981) Some relationships between the biochemistry of photosynthesis and the gas exchange of leaves. Planta **153:** 376–387

Walker GH, Edwards GE (1990) Inhibition of maize leaf phosphoenolpyruvate carboxylase by diethyl oxaloacetate. Photosynth Res **25:** 101–106

Walker GH, Ku MSB, Edwards GE (1986) Activity of maize leaf phosphoenolpyruvate carboxylase in relation to tautomerization and nonenzymatic decarboxylation of oxaloacetate. Arch Biochem Biophys **248:** 489–501

Wedding RT, Black MK (1986) Malate inhibition of phosphoenolpyruvate carboxylase from *Crassula*. Plant Physiol **82:** 985–990

Wedding RT, Black MK, Meyer CR (1990) Inhibition of phosphoenolpyruvate carboxylase by malate. Plant Physiol **92:** 456–461

Weise SE, Li Z, Sutter AE, Corrion A, Banerjee A, Sharkey TD (2013) Measuring dimethylallyl diphosphate available for isoprene synthesis. Anal Biochem **435:** 27–34

Wiberley AE, Linskey AR, Falbel TG, Sharkey TD (2005) Development of the capacity for isoprene emission in kudzu. Plant Cell Environ **28:** 898–905

Wilkinson MJ, Monson RK, Trahan N, Lee S, Brown E, Jackson RB, Polley HW, Fay PA, Fall R (2009) Leaf isoprene emission rate as a function of atmospheric CO_2 concentration. Glob Change Biol **15:** 1189–1200

Yu Q, Liu J, Wang Z, Nai J, Lü M, Zhou X, Cheng Y (2013) Characterization of the NADP-malic enzymes in the woody plant *Populus trichocarpa*. Mol Biol Rep **40:** 1385–1396